Integrazione geostatistica di dati con applicazioni a modelli idrogeologici a scala regionale

Giulio Vignoli, University of Cagliari, Cagliari, ITA / GEUS, Aarhus, DK
Anne-Sophie Høyer, GEUS, Aarhus, DK
Thomas Mejer Hansen, Aarhus University, Aarhus, DK
Le Thanh Vu, I-GIS, Aarhus, DK
Donald A. Keefer, ISGS, Chicago, USA
Flemming Jørgensen, Central Denmark Region, Viborg, DK

GNGTS 2018 Bologna, Italia

Outline

- The problem (the study area)
- The development of the Training Image
- The hard conditioning
- The soft conditioning strategy
- Comparison of the realizations
- Conclusions

The study area

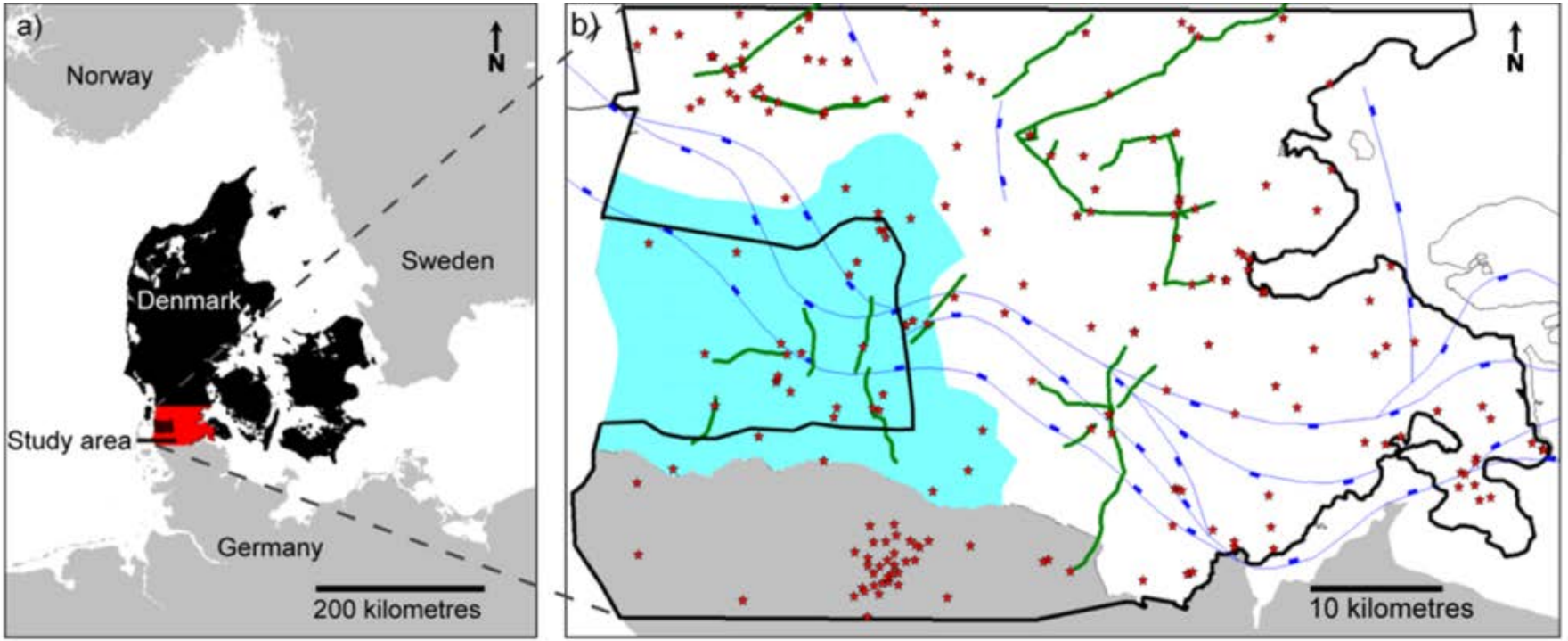

The Training Image development

Training Images

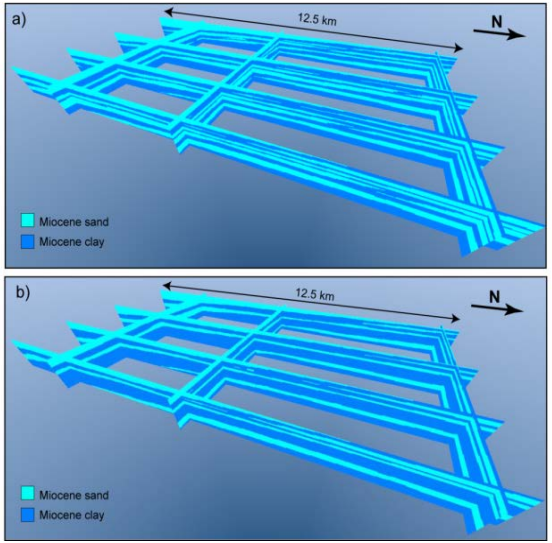

Unconstrained realization

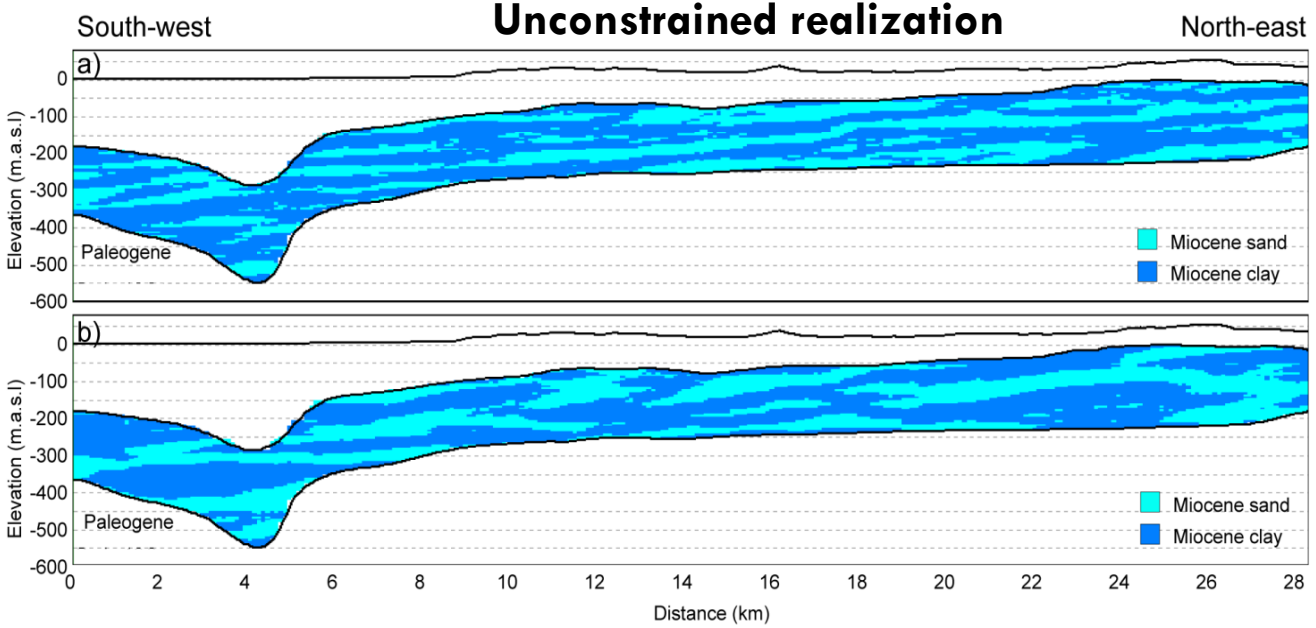

The Training Image development

Training Images

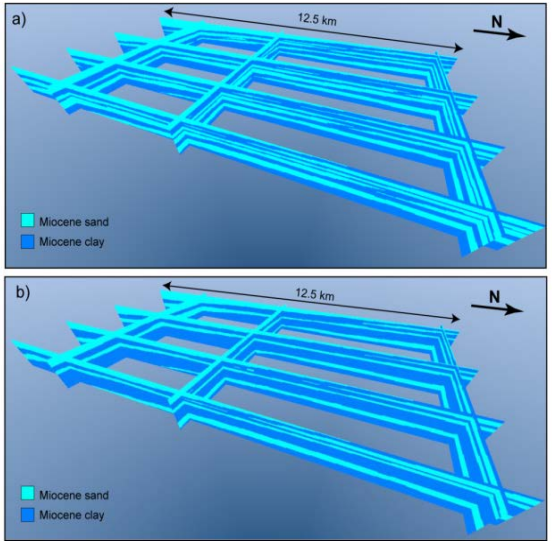

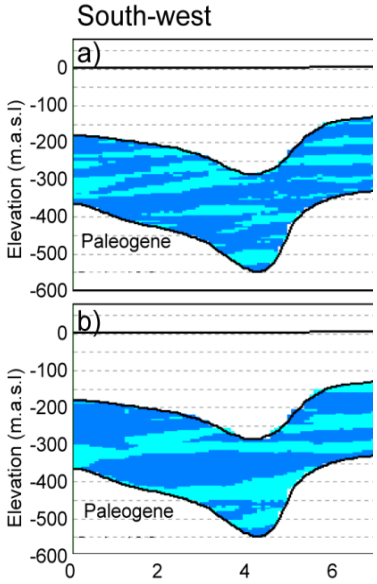

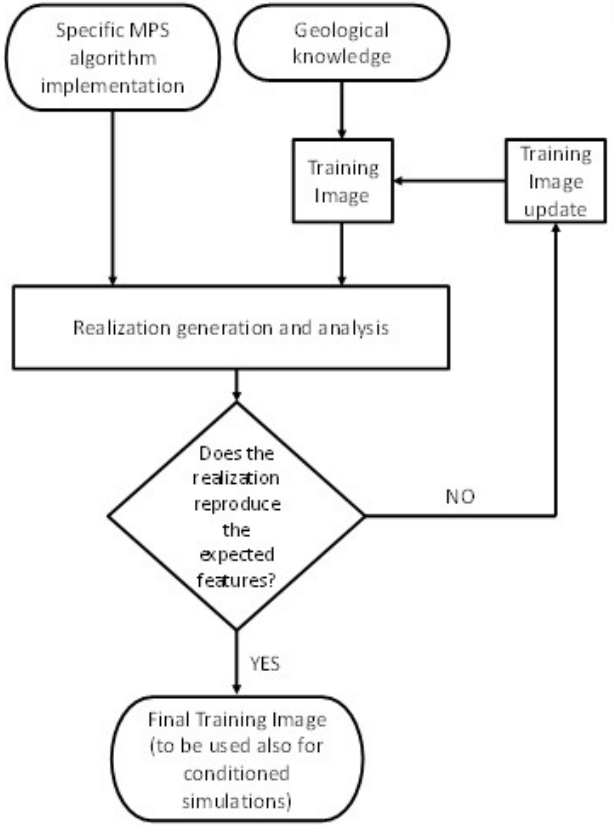

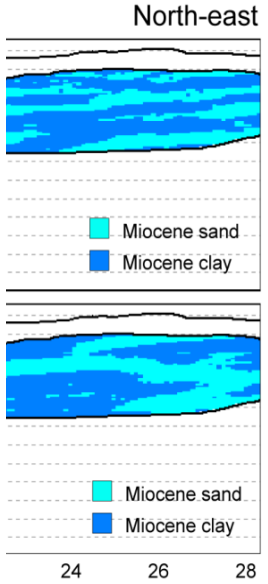

The **hard conditioning** data

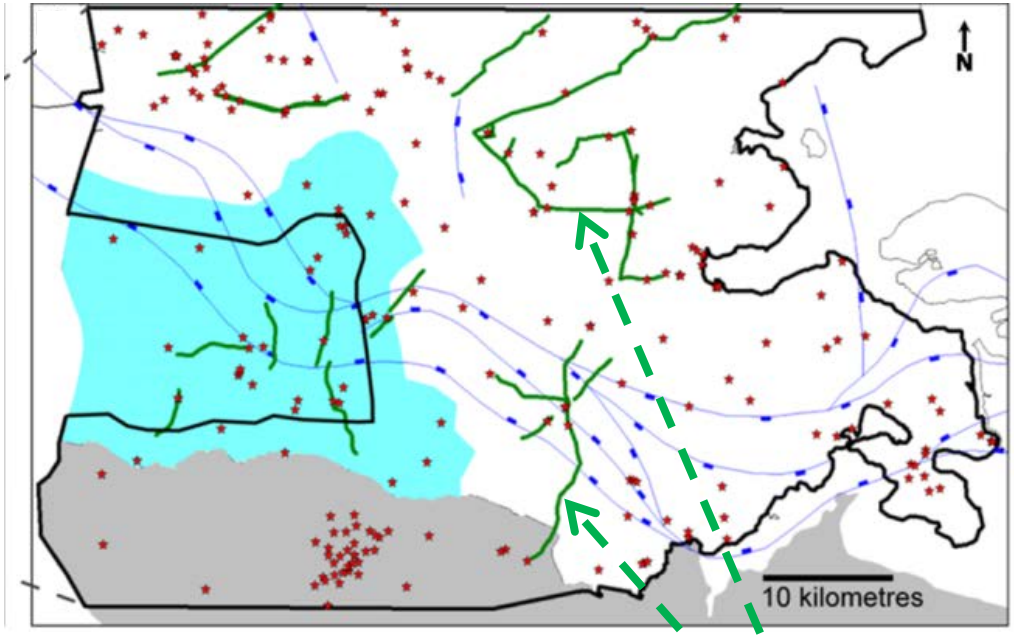

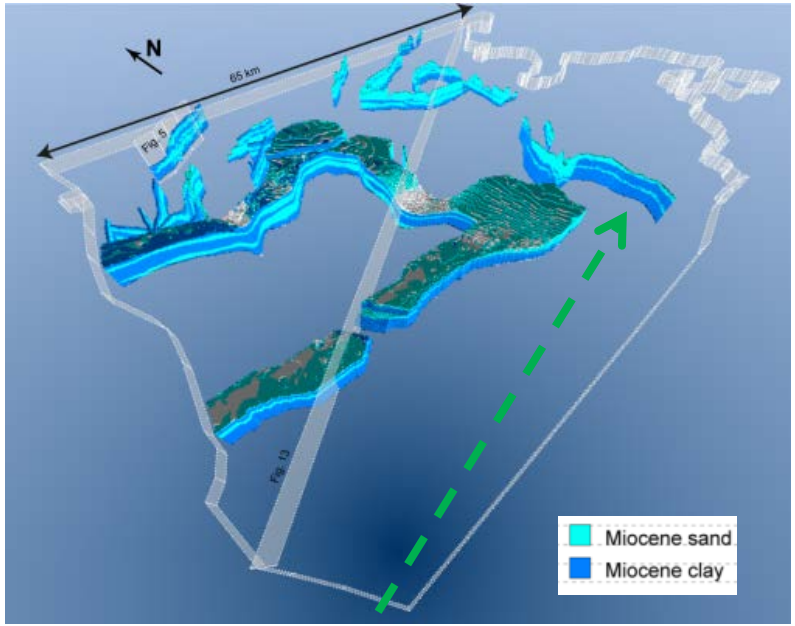

The **seismic lines**

The hard conditioning data

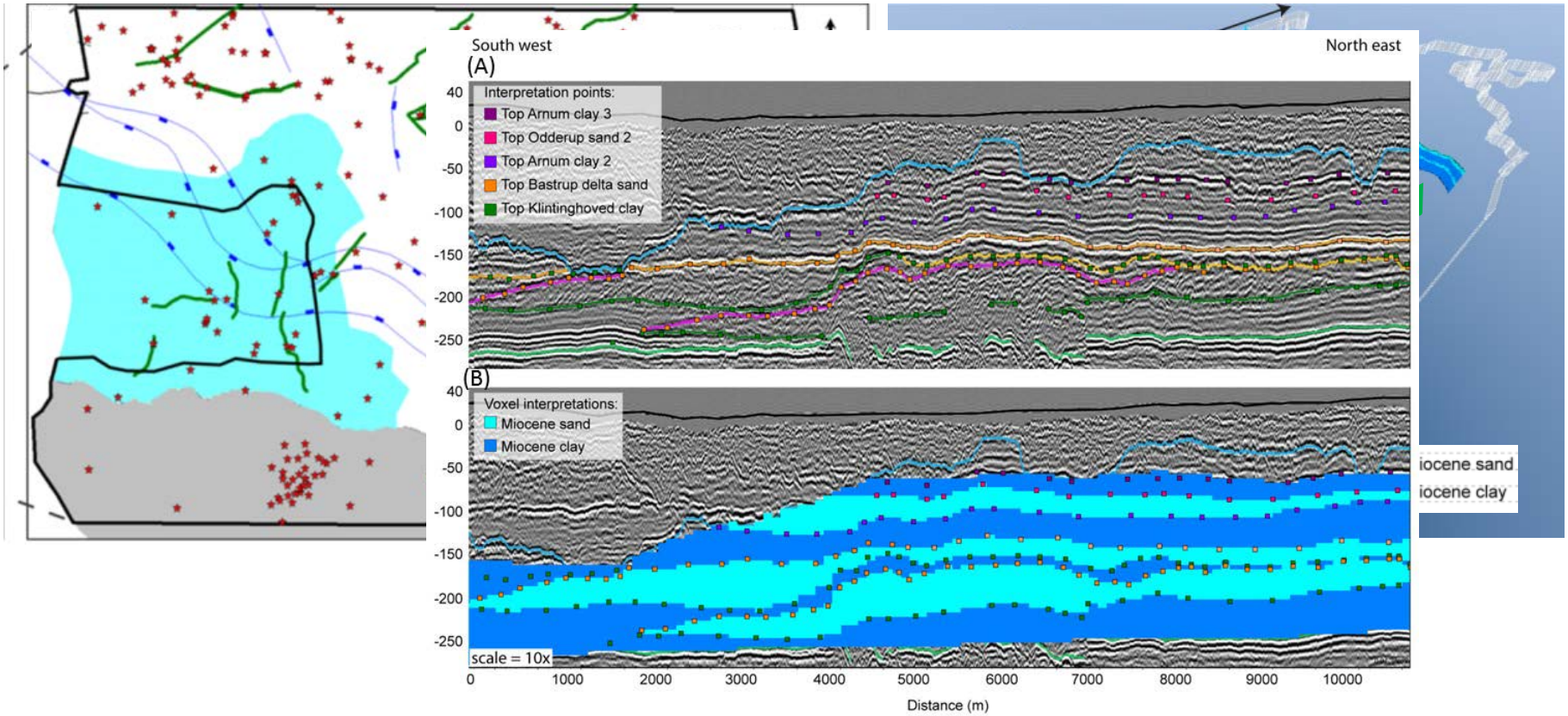

The **hard conditioning** data

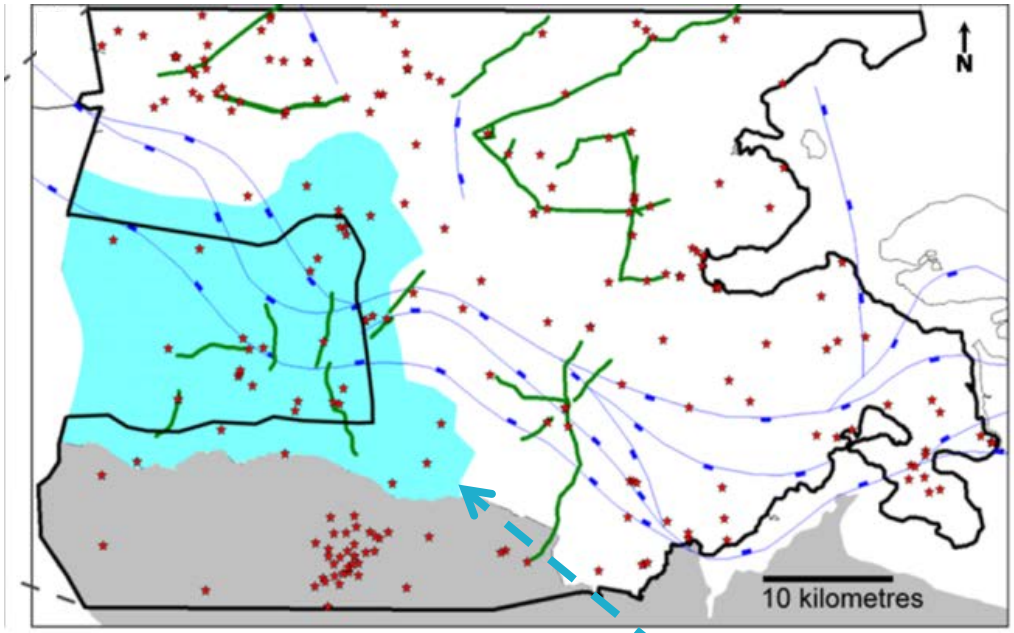

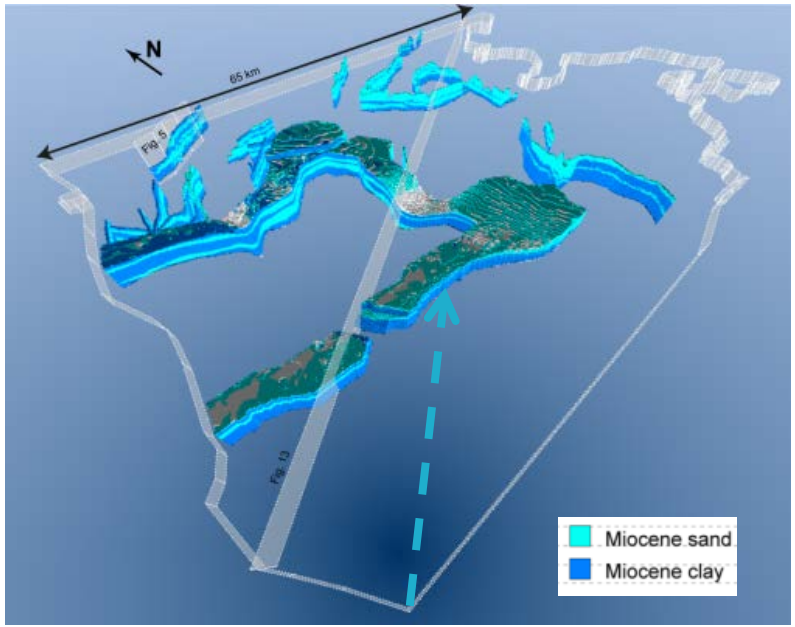

The **pre-existing model**

The soft conditioning data

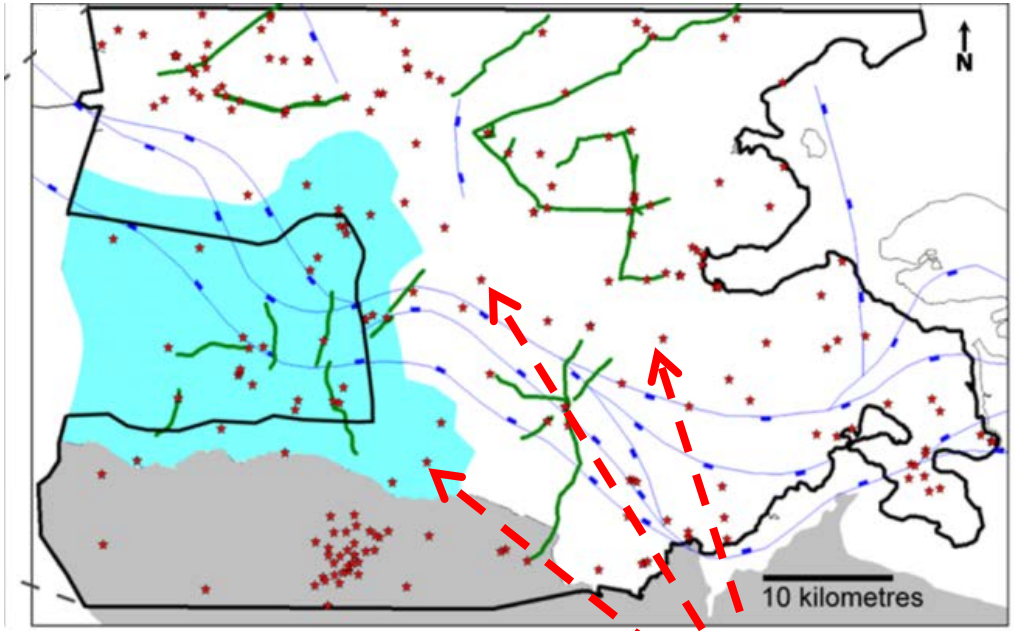

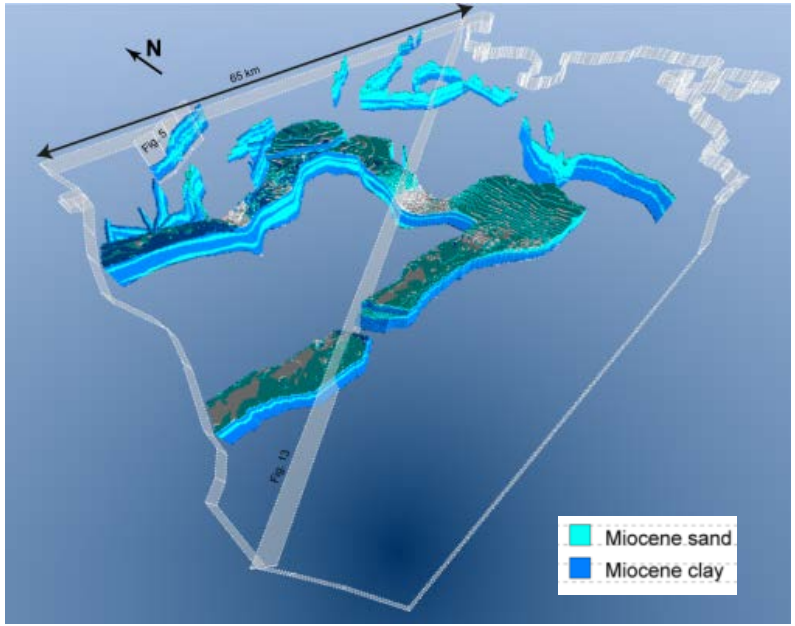

The borehole locations

The soft conditioning data

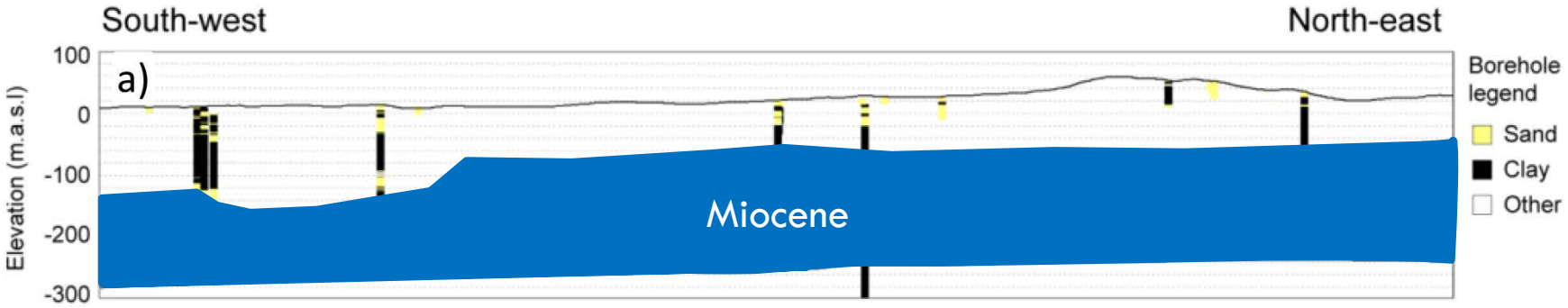

The soft conditioning strategy

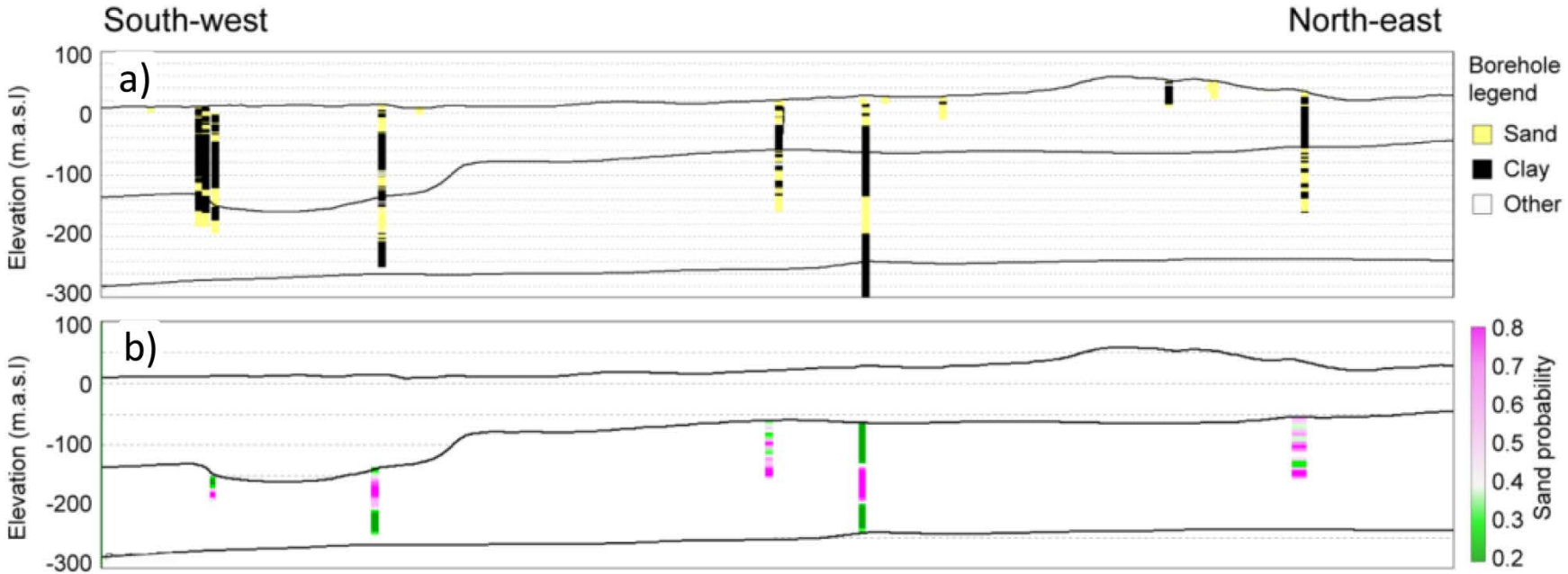

The soft conditioning strategy

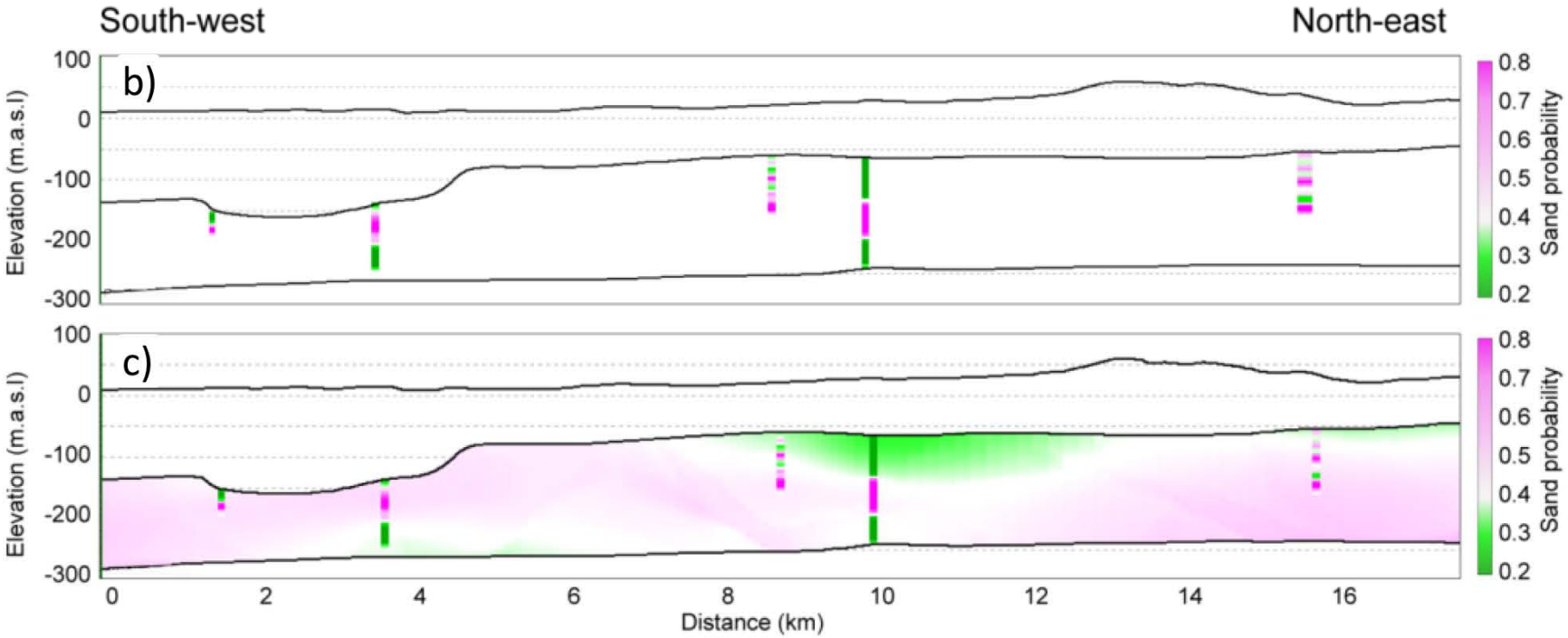

The soft conditioning strategy

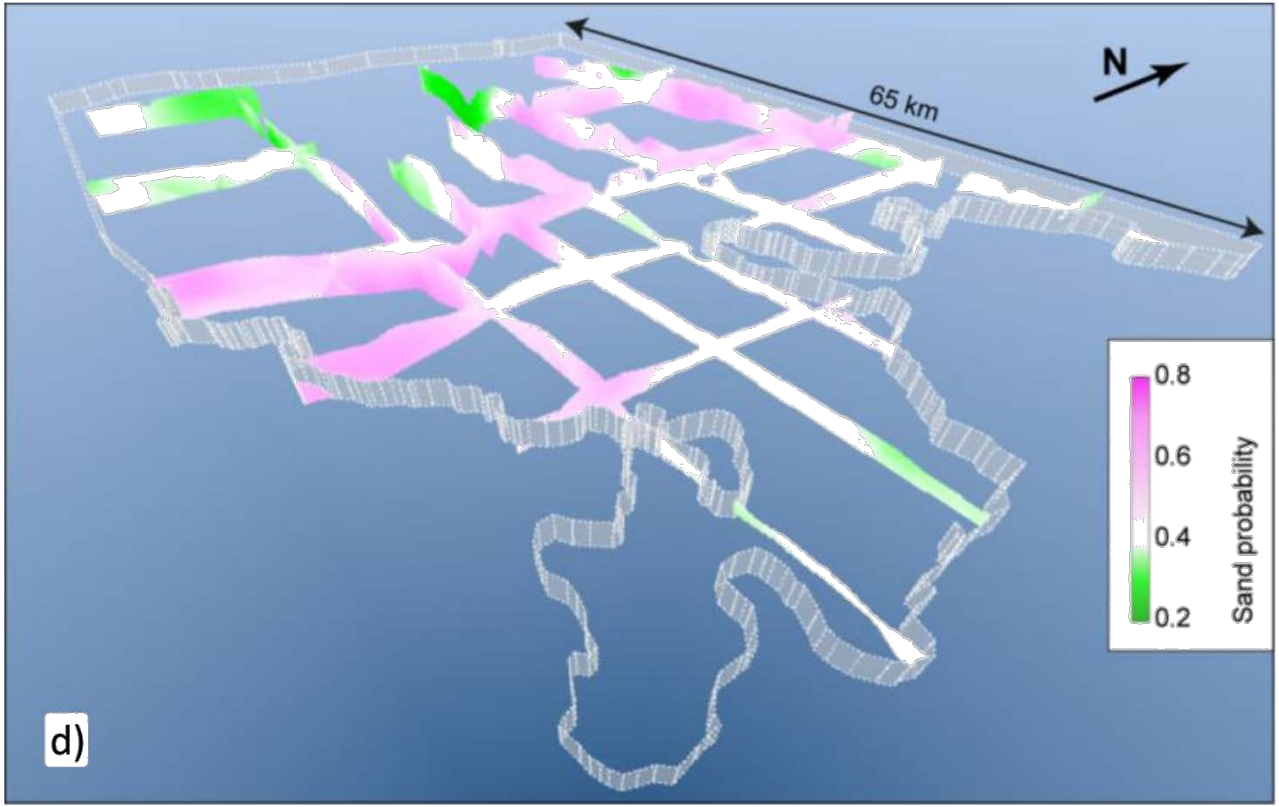

The soft conditioning strategy

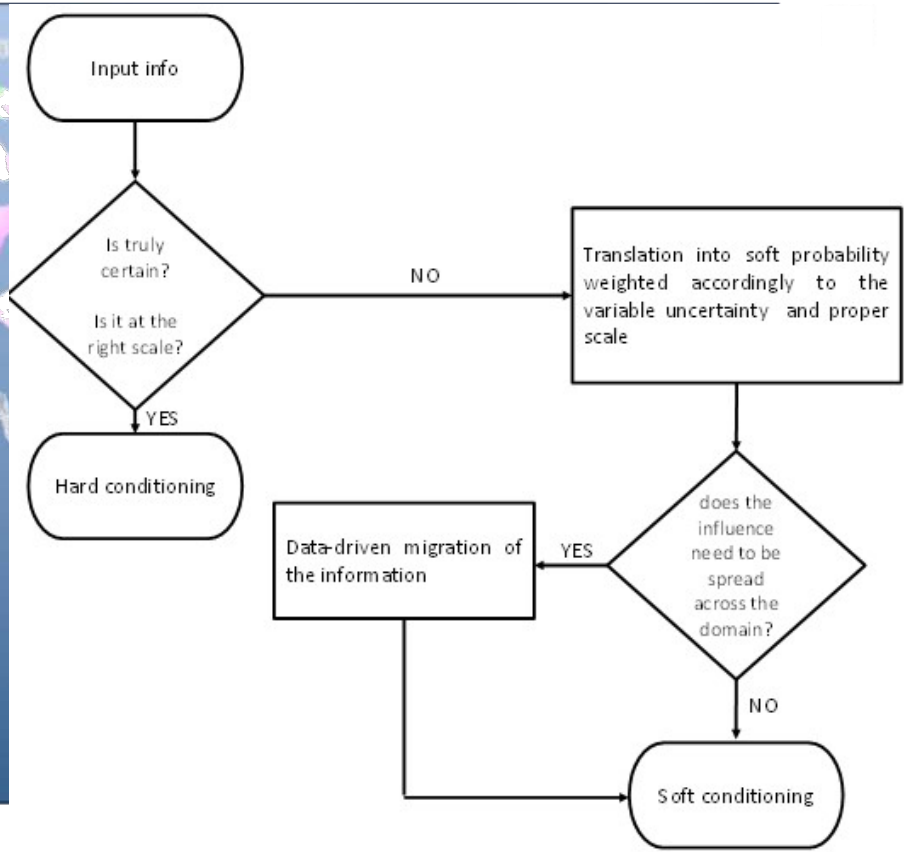

The realizations

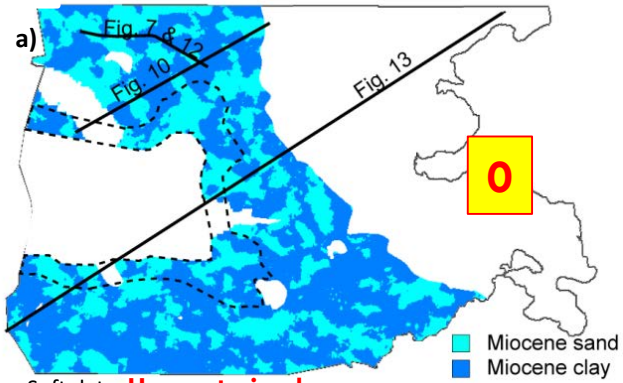

Soft data: **Unconstrained**

Hard data: ÷

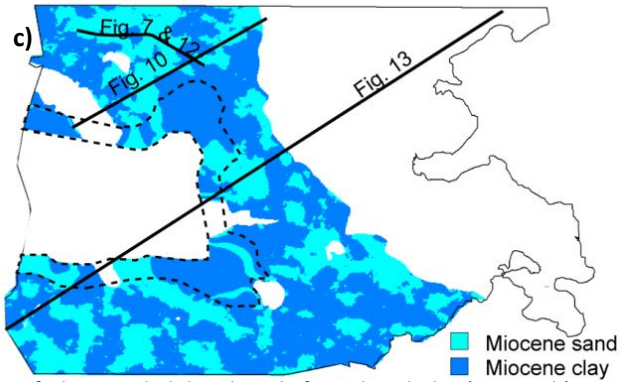

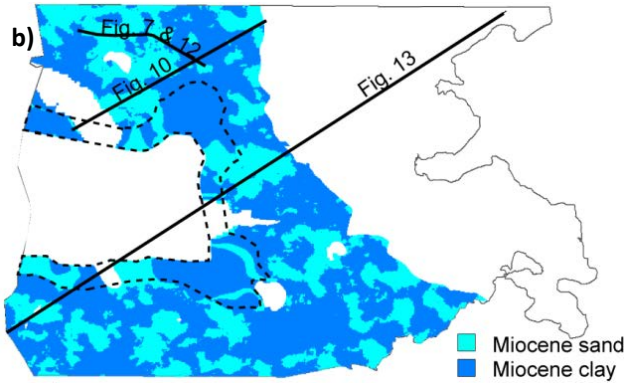

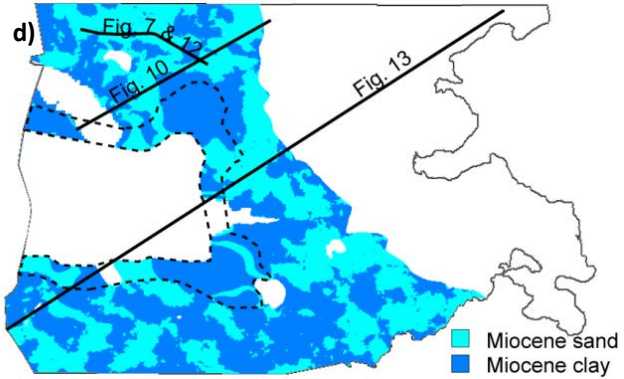

The realizations

a)

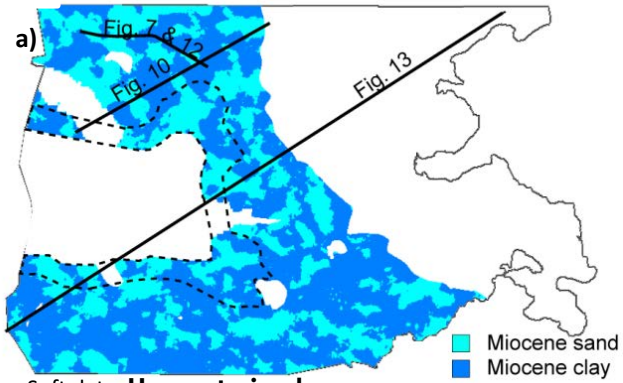

Soft data: **Unconstrained**

Hard data: ÷

c)

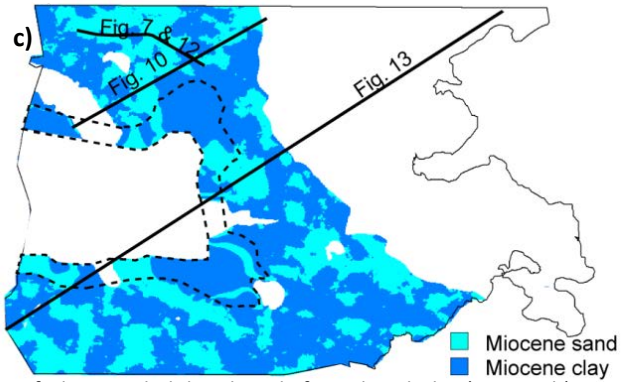

b)

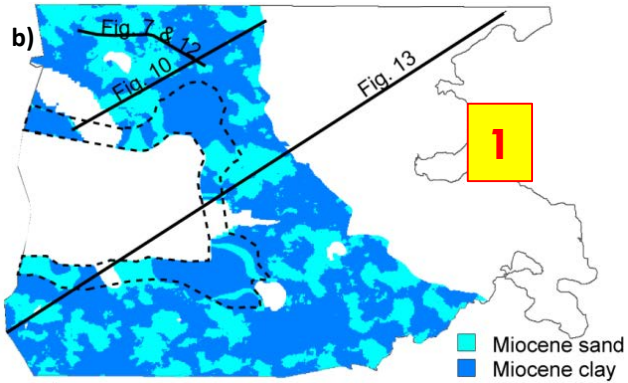

Soft data:

Hard data: **Tønder model, Seismic lines, Boreholes**

d)

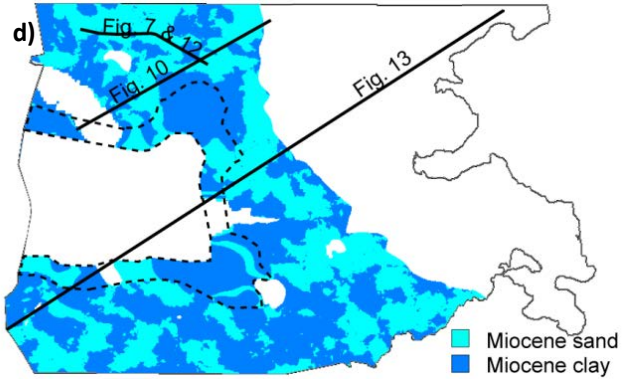

The realizations

a)

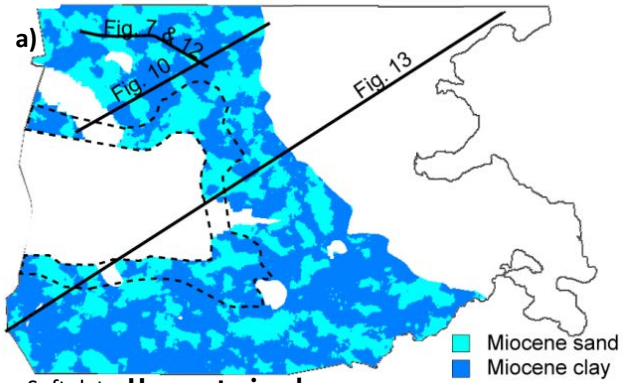

Soft data: **Unconstrained**

Hard data: ÷

c)

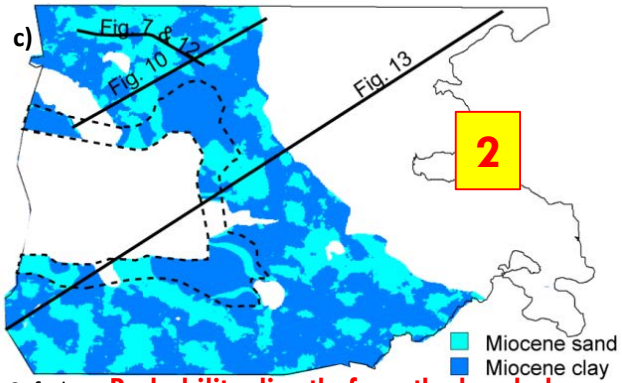

Soft data: **Probability directly from the boreholes**

Hard data: **Tønder model, Seismic lines**

b)

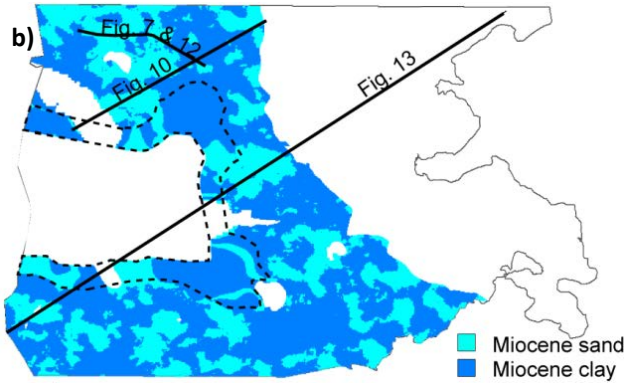

Soft data:

Hard data: **Tønder model, Seismic lines, Boreholes**

d)

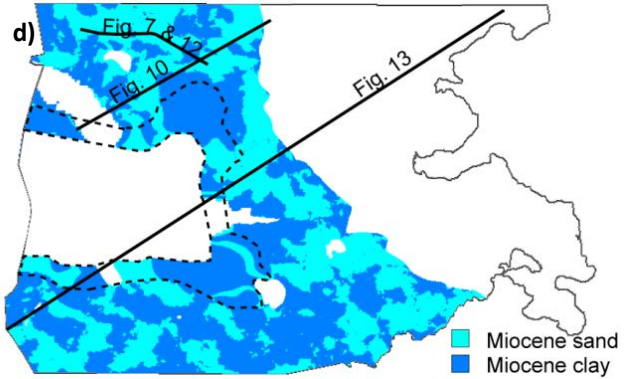

The realizations

a)

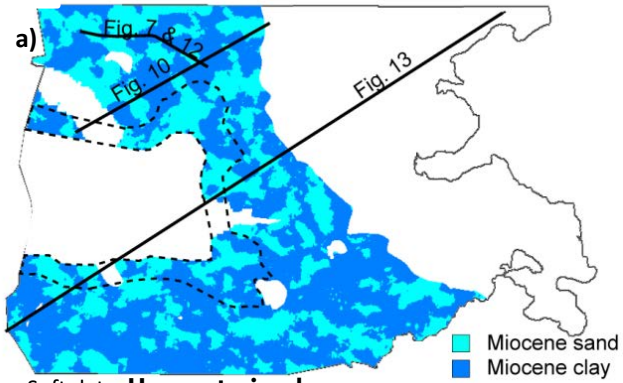

Soft data: **Unconstrained**
Hard data: ÷

c)

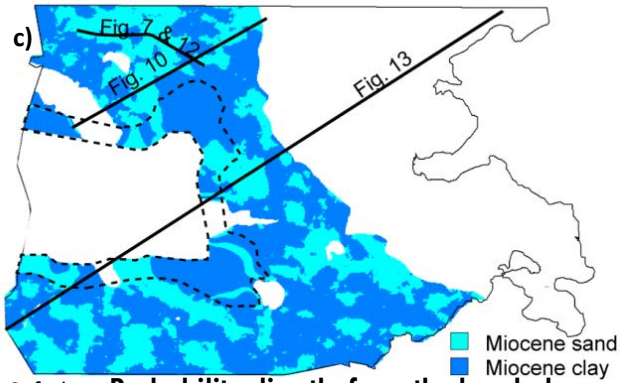

Soft data: **Probability directly from the boreholes**
Hard data: **Tønder model, Seismic lines**

b)

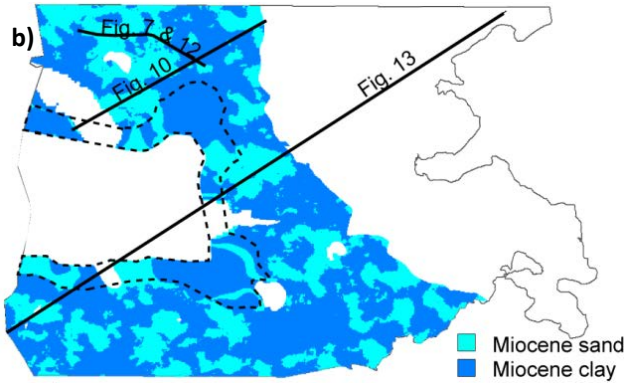

Soft data:
Hard data: **Tønder model, Seismic lines, Boreholes**

d)

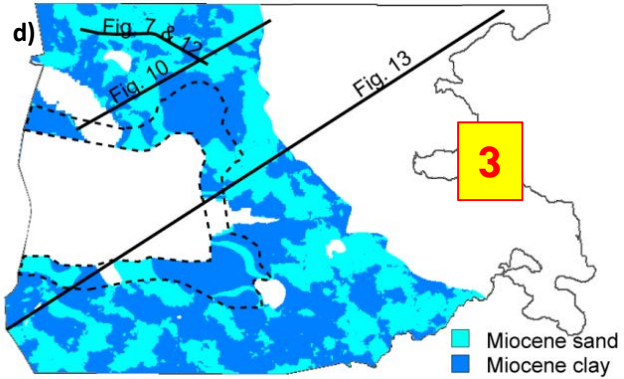

Soft data: **3D probability kriged from the boreholes**
Hard data: **Tønder model, Seismic lines**

The realizations

a)

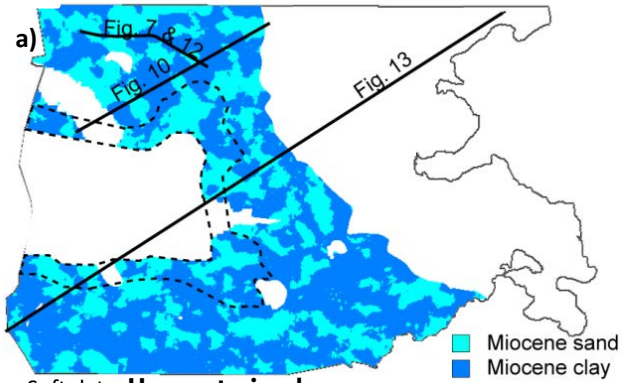

Soft data: **Unconstrained**
Hard data: ÷

c)

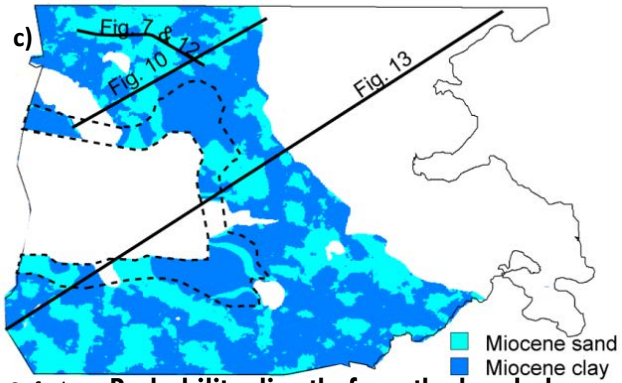

Soft data: **Probability directly from the boreholes**
Hard data: **Tønder model, Seismic lines**

b)

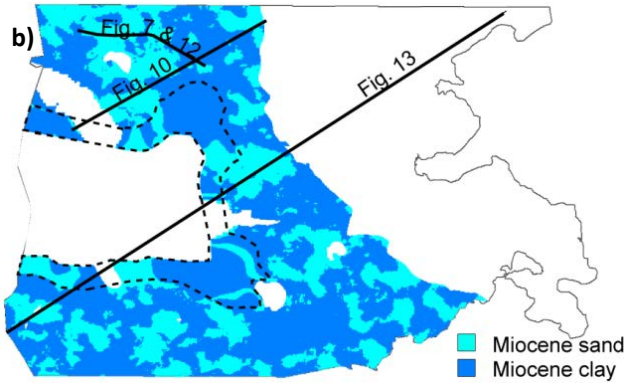

Soft data:
Hard data: **Tønder model, Seismic lines, Boreholes**

d)

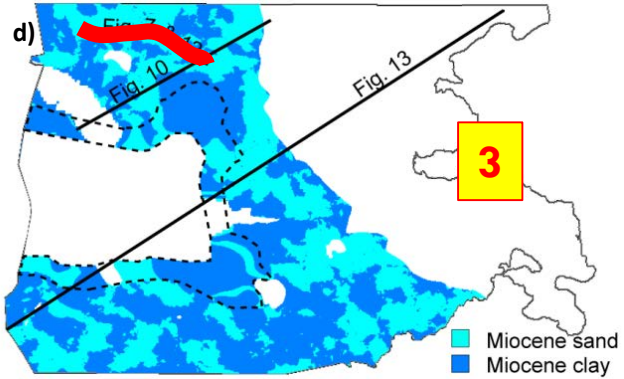

Soft data: **3D probability kriged from the boreholes**
Hard data: **Tønder model, Seismic lines**

The realizations

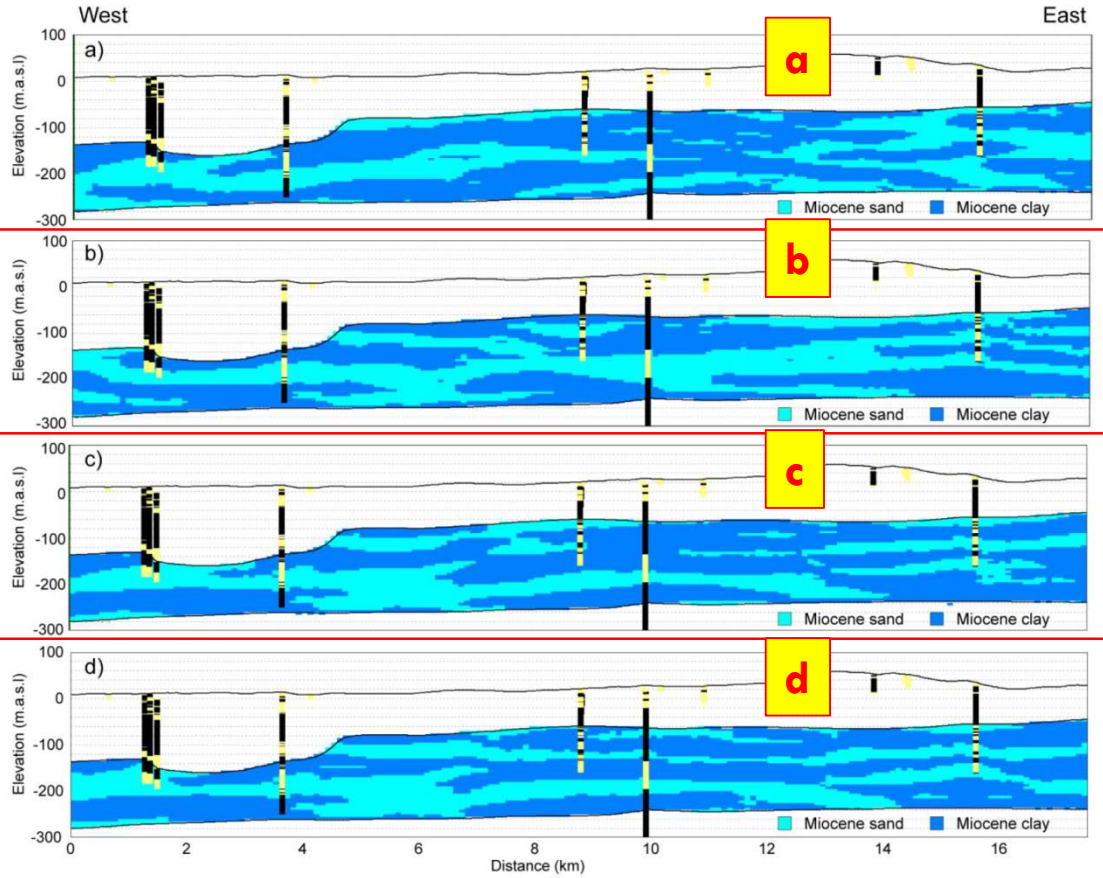

a — **Unconstrained**

b — **Hard data:**
Tønder model, Seismic lines, Boreholes

c — **Soft data: Probability directly from the boreholes**

Hard data: Tønder model, Seismic lines

d — **Soft data: 3D probability kriged from the boreholes**

Hard data: Tønder model, Seismic lines

The realizations

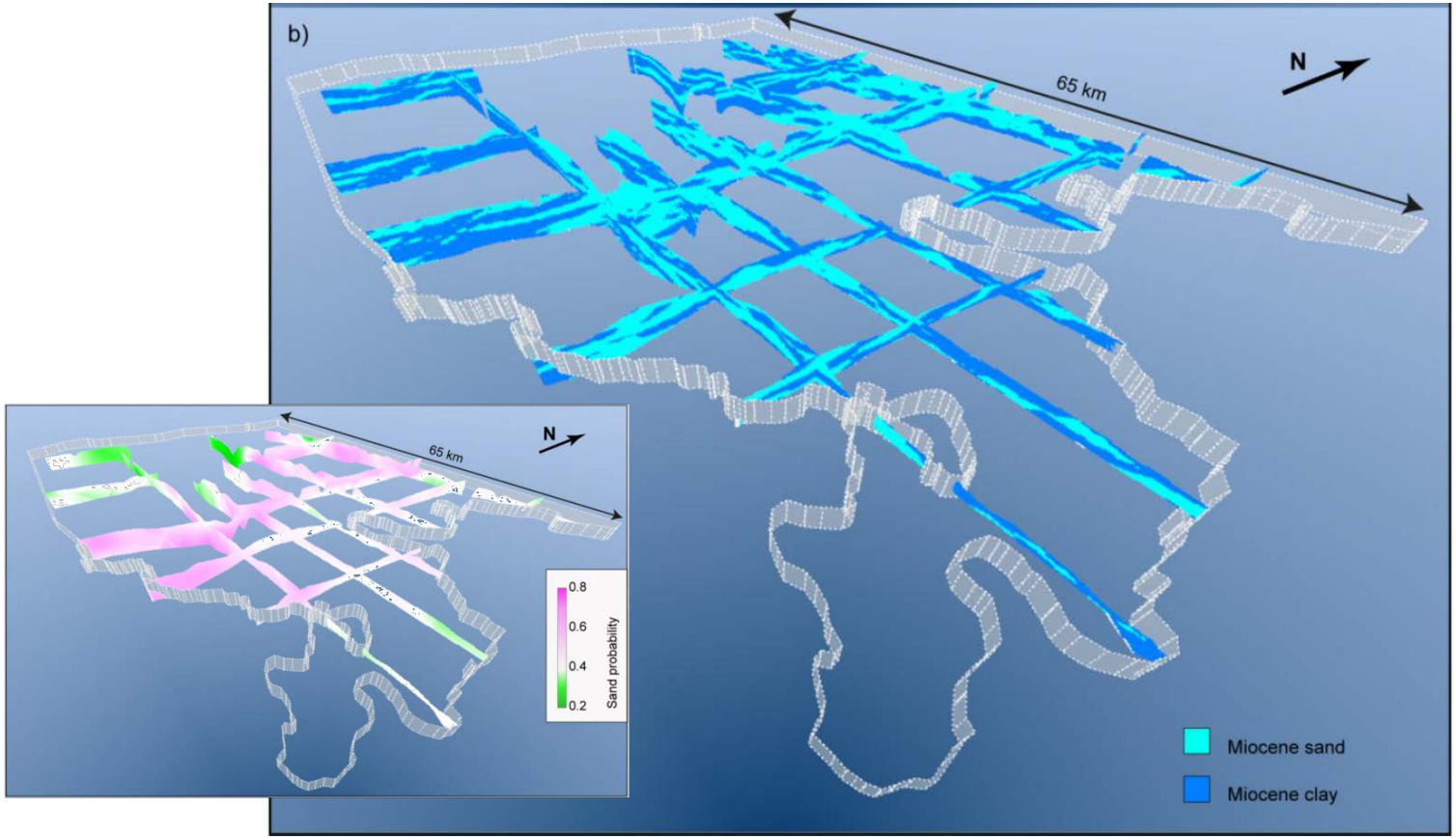

Conclusions

- This study investigates strategies for MPS simulations in large 3D model domains consistent with different types of input data. The strategies were tested within an area of 2 810 km^2 in which the Miocene unit was modelled using MPS simulation.
- The final TI was developed iteratively by checking the outcomes of the corresponding unconditioned simulations, and adjusting it in order to obtain the most geologically meaningful structures in the final realizations. Inherently, this approach takes into account the effects of the specific MPS implementation used.
- The previously published Tønder model and reliable seismic interpretations were used as hard conditioning data in order to preserve the associated information during the simulation.
- The boreholes (more uncertain, and characterized by a different scale with respect to the simulation) have been translated into soft probability via a moving window strategy.

Conclusions

- **SNESIM limits the influence of soft conditioning data to local neighbourhoods around each data value and is unable to effectively migrate the information, for example, far from the boreholes.**
  A straightforward and effective strategy to address this problem consists in kriging the sand probability derived from the boreholes into a 3D voxel model and using it as soft conditioning.

https://www.hydrol-earth-syst-sci.net/21/6069/2017/hess-21-6069-2017.html

Hydrol. Earth Syst. Sci., 21, 6069–6089, 2017
https://doi.org/10.5194/hess-21-6069-2017

Hydrology and Earth System Sciences
Open Access
EGU

https://www.sciencedirect.com/science/article/pii/S0022169418303470

Journal of Hydrology 562 (2018) 544–563

Contents lists available at ScienceDirect

Journal of Hydrology

journal homepage: www.elsevier.com/locate/jhydrol

Research papers

Regional flow in a complex coastal aquifer system: Combining voxel geological modelling with regularized calibration

Rena Meyer[a,*], Peter Engesgaard[a], Anne-Sophie Høyer[b], Flemming Jørgensen[b], Giulio Vignoli[b,c], Torben O. Sonnenborg[b]

[a] Department of Geosciences and Natural Resource Management (IGN), University of Copenhagen, Denmark
[b] Geological Survey of Denmark and Greenland (GEUS), Denmark
[c] Dipartimento di Ingegneria Civile, Ambientale e Architettura (DICAAR), Università di Cagliari, Italy

Multiple-point statistical simulation for hydrogeological models: 3-D training image development and conditioning strategies

Anne-Sophie Høyer[1], Giulio Vignoli[1,2], Thomas Mejer Hansen[3], Le Thanh Vu[4], Donald A. Keefer[5], and Flemming Jørgensen[1]

[1]Groundwater and Quaternary Geology Mapping Department, GEUS, Aarhus, 8000, Denmark
[2]Department of Civil, Environmental Engineering and Architecture (DICAAR), University of Cagliari, Cagliari, 09123, Italy
[3]Niels Bohr Institute, University of Copenhagen, Copenhagen, 2100, Denmark
[4]I-GIS, Risskov, 8240, Denmark
[5]Illinois State Geological Survey, Prairie Research Institute, University of Illinois, Champaign, Illinois 61820, USA

Correspondence to: Anne-Sophie Høyer (ahc@geus.dk) and Giulio Vignoli (gvignoli@unica.it)

Received: 1 November 2016 – Discussion started: 25 November 2016
Revised: 12 October 2017 – Accepted: 17 October 2017 – Published: 1 December 2017

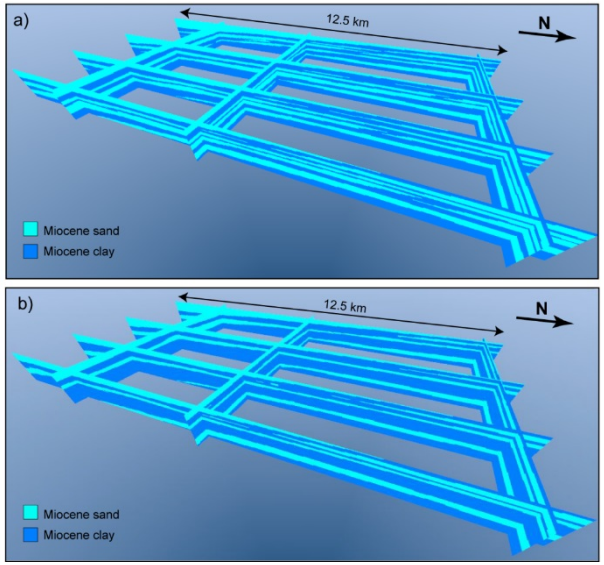

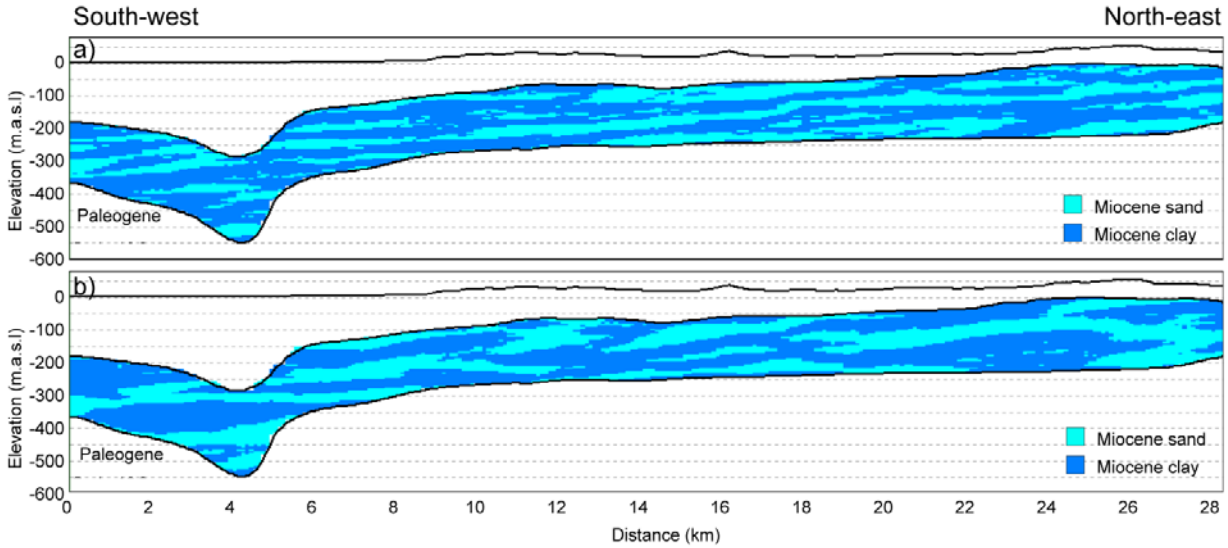

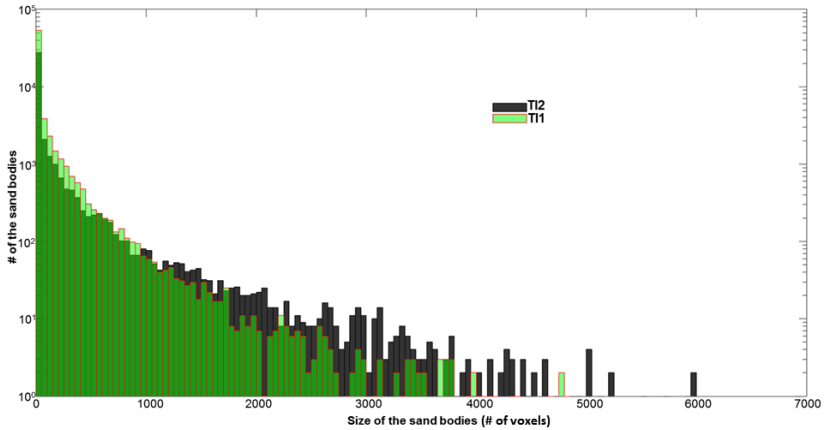

Sizes of the sand bodies of the unconditioned realizations

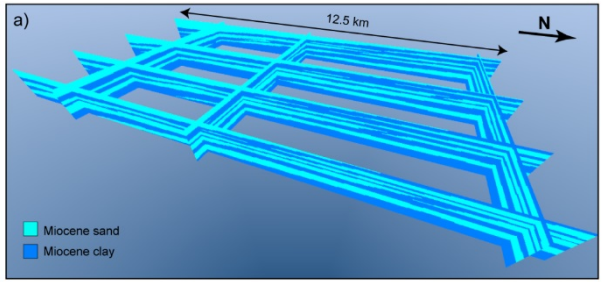

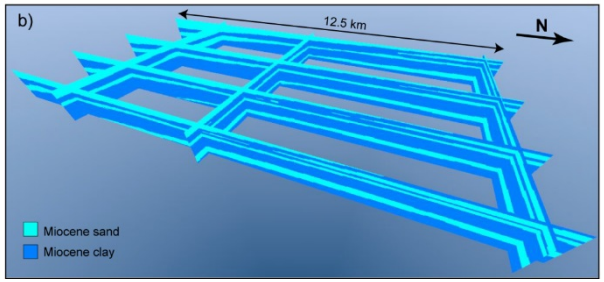

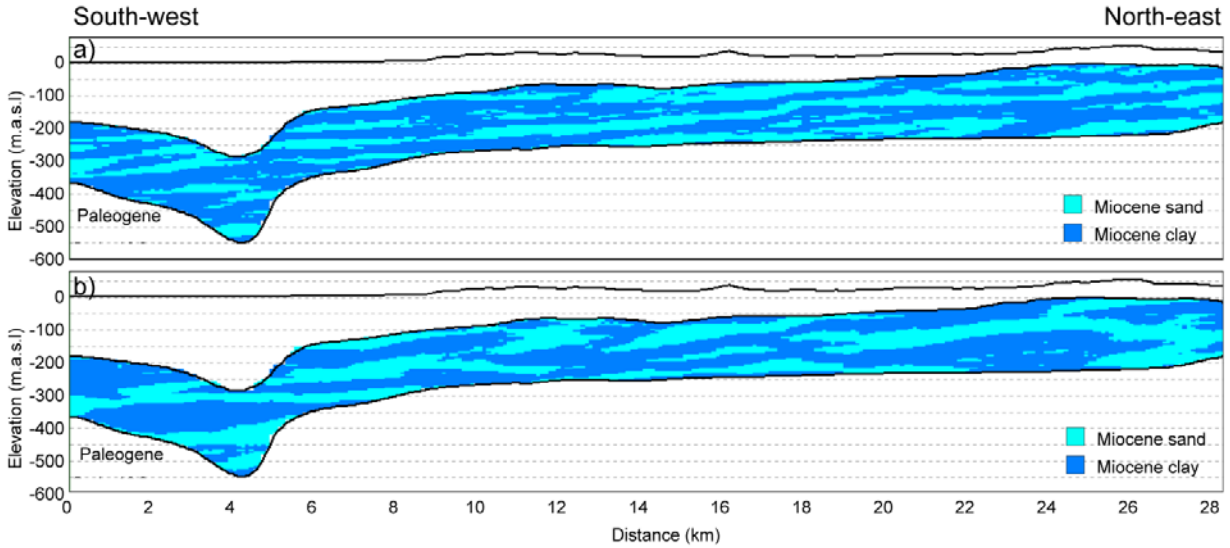

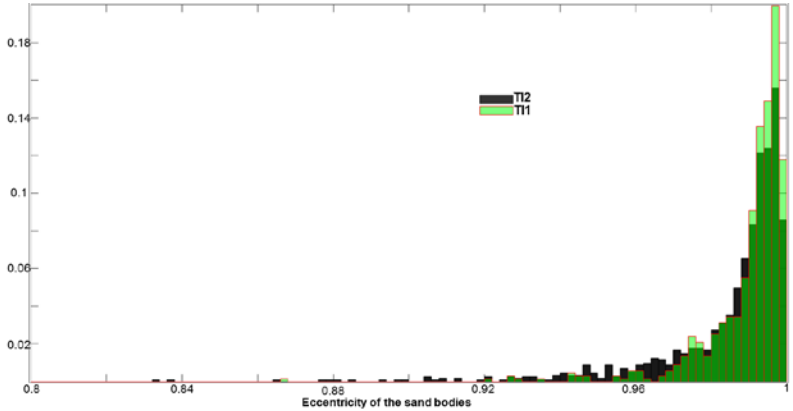

Probability of the eccentricity of the sand bodies (with a size larger than 1000) for the unconditioned realizations

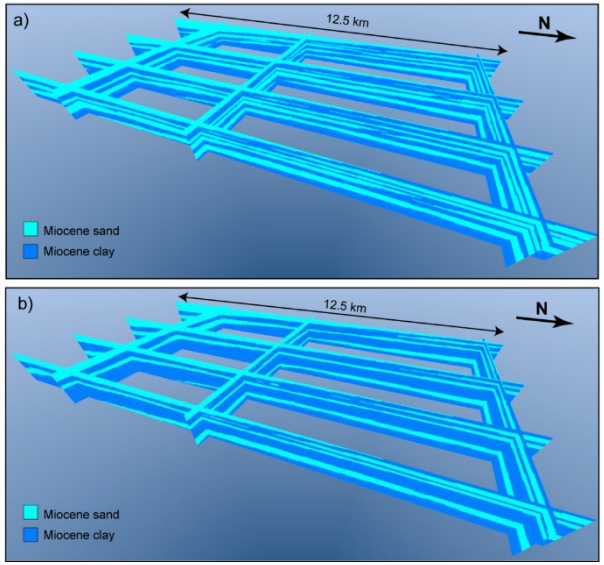

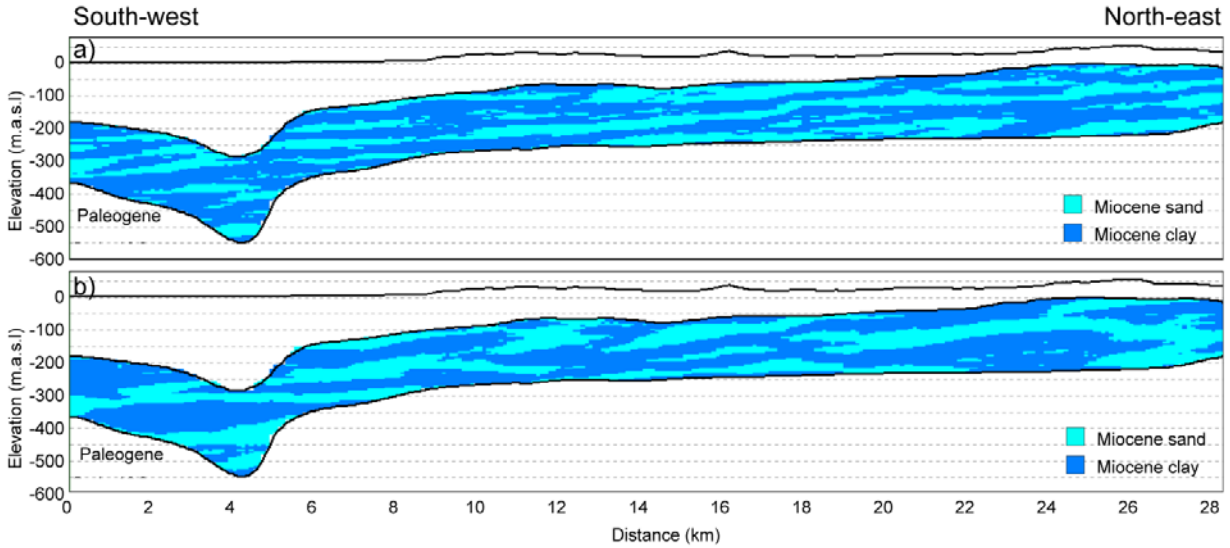

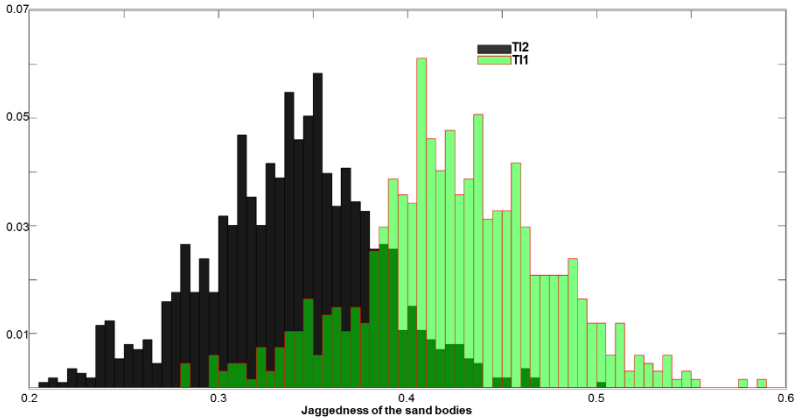

Probability of the jaggedness (the ratio between the surface and the size of the bodies) of the sand bodies (with a size larger than 1000) for the unconditioned realizations

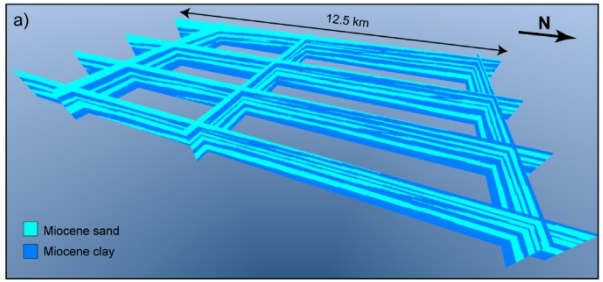
a)
12.5 km
N
Miocene sand
Miocene clay

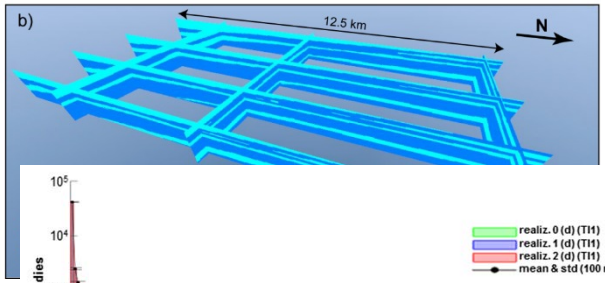
b)
12.5 km
N

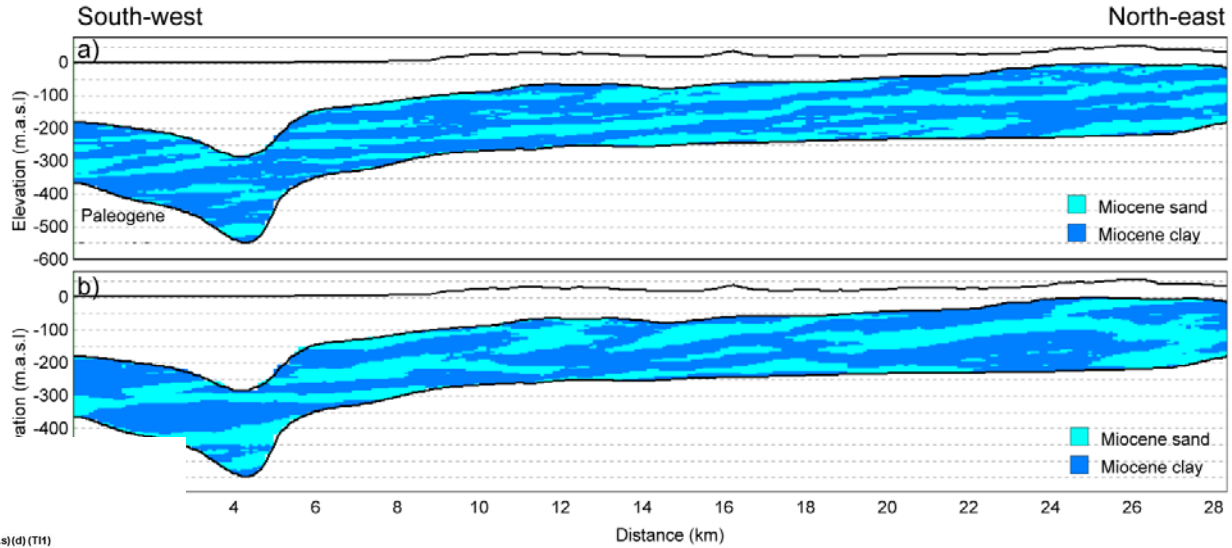
South-west
North-east
a)
b)
Elevation (m.a.s.l)
Paleogene
Miocene sand
Miocene clay
Distance (km)

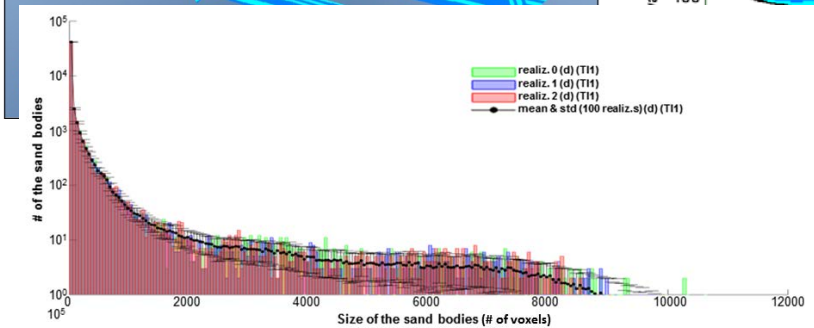
of the sand bodies
realiz. 0 (d) (TI1)
realiz. 1 (d) (TI1)
realiz. 2 (d) (TI1)
mean & std (100 realiz.s) (d) (TI1)
Size of the sand bodies (# of voxels)

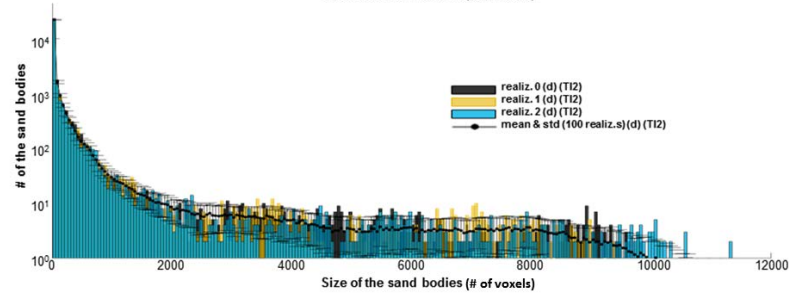
of the sand bodies
realiz. 0 (d) (TI2)
realiz. 1 (d) (TI2)
realiz. 2 (d) (TI2)
mean & std (100 realiz.s) (d) (TI2)
Size of the sand bodies (# of voxels)

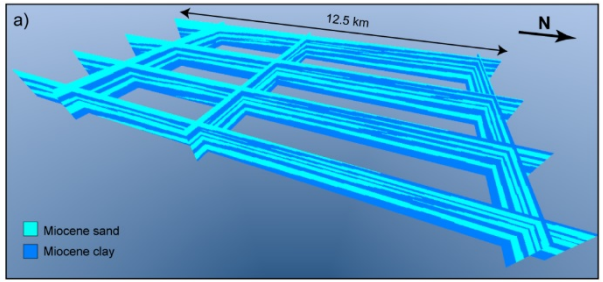
a)
12.5 km
N
Miocene sand
Miocene clay

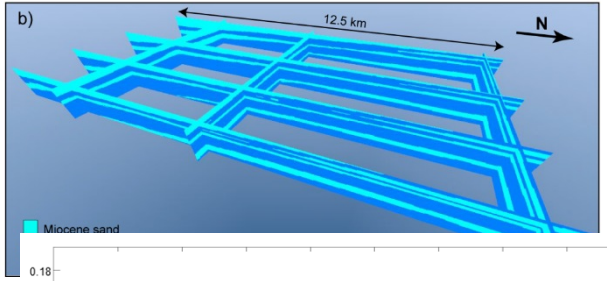
b)
12.5 km
N
Miocene sand

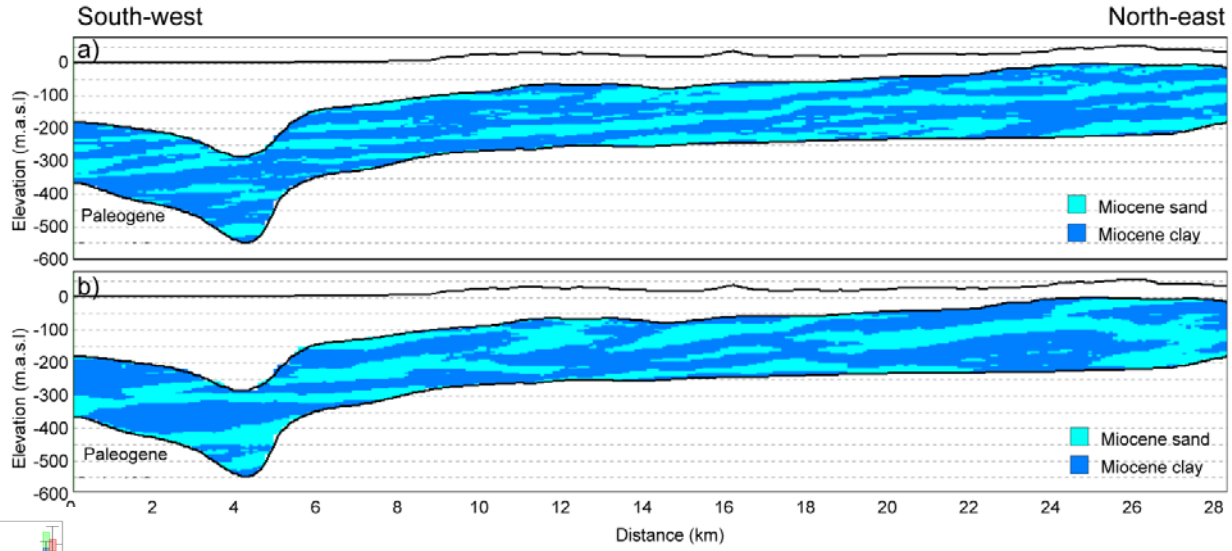
South-west
North-east
a)
b)
Elevation (m.a.s.l)
0
-100
-200
-300
-400
-500
-600
Paleogene
Miocene sand
Miocene clay
2
4
6
8
10
12
14
16
18
20
22
24
26
28
Distance (km)

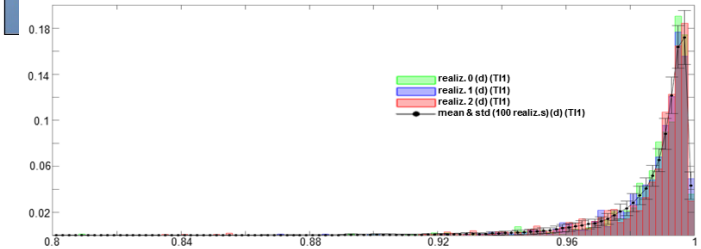
0.18
0.14
0.1
0.06
0.02
realiz. 0 (d) (TI1)
realiz. 1 (d) (TI1)
realiz. 2 (d) (TI1)
mean & std (100 realiz.s) (d) (TI1)
0.8
0.84
0.88
0.92
0.96
1

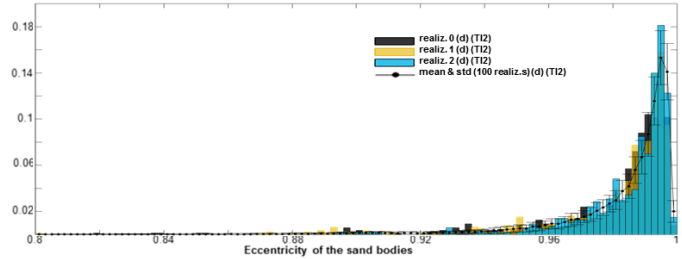
0.18
0.14
0.1
0.06
0.02
realiz. 0 (d) (TI2)
realiz. 1 (d) (TI2)
realiz. 2 (d) (TI2)
mean & std (100 realiz.s) (d) (TI2)
0.8
0.84
0.88
0.92
0.96
1
Eccentricity of the sand bodies

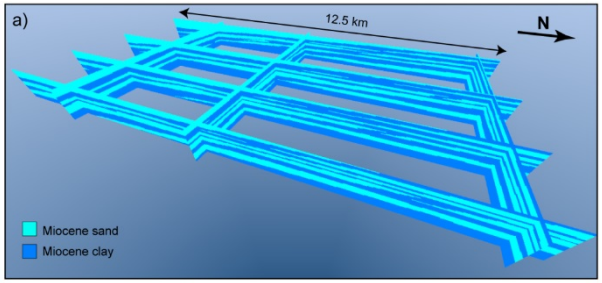
a)
12.5 km
N
Miocene sand
Miocene clay

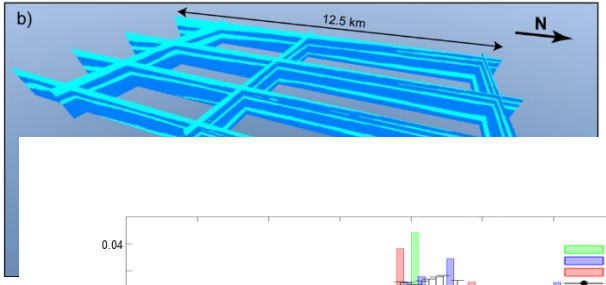
b)
12.5 km
N

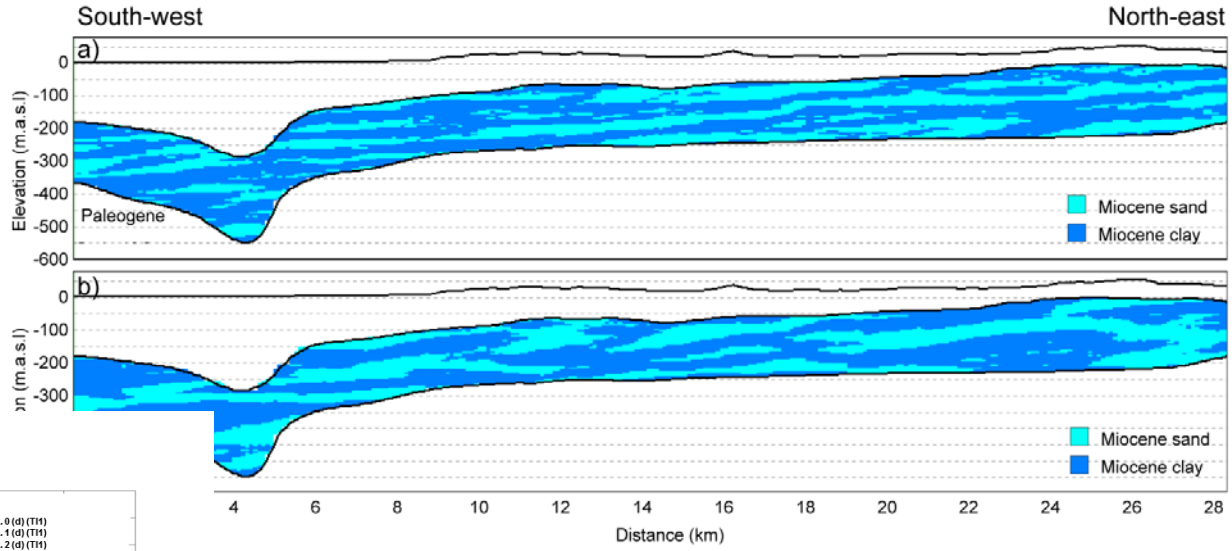
South-west
North-east
a)
b)
Elevation (m.a.s.l)
Paleogene
Miocene sand
Miocene clay
Distance (km)

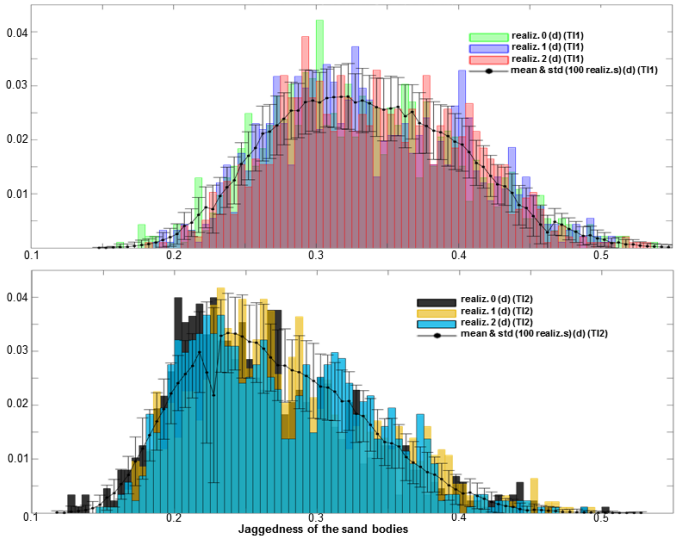
realiz. 0 (d) (TI1)
realiz. 1 (d) (TI1)
realiz. 2 (d) (TI1)
mean & std (100 realiz.s) (d) (TI1)
realiz. 0 (d) (TI2)
realiz. 1 (d) (TI2)
realiz. 2 (d) (TI2)
mean & std (100 realiz.s) (d) (TI2)
Jaggedness of the sand bodies

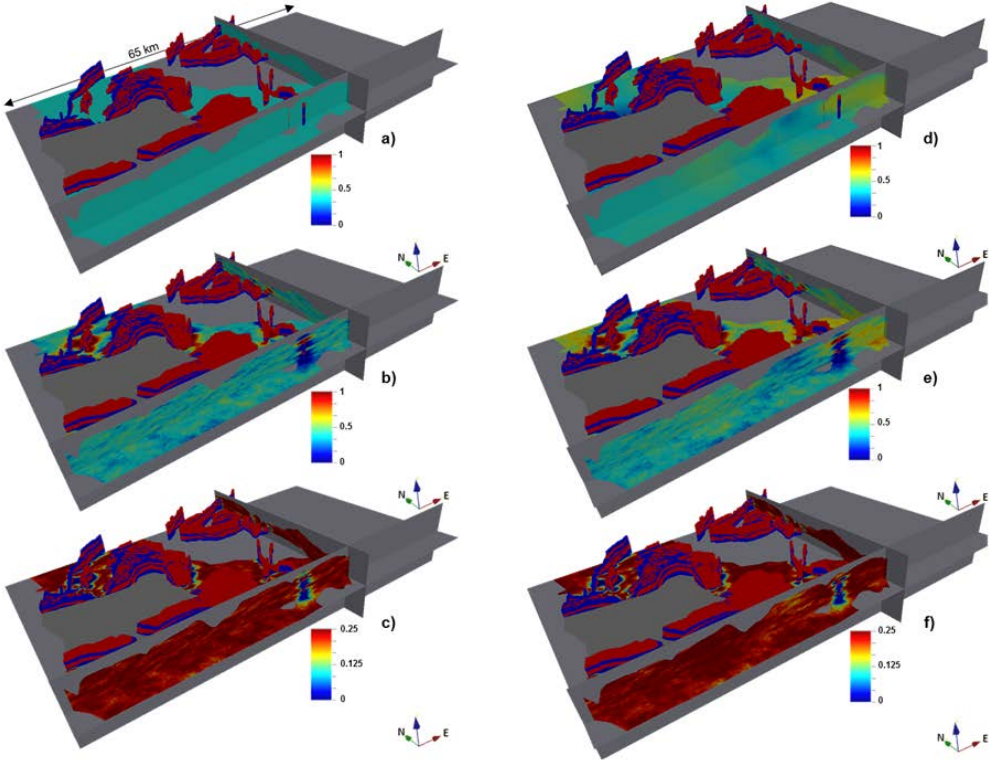

Comparison of the conditioning approaches characterized by boreholes as soft conditioning:
soft and hard conditioning - panels (a) and (d);
e-type map - panels (b) and (e);
variance map - panels (c) and (f).

To facilitate the comparison, the probabilities in panels (a) and (d) are presented in a different colour scale with respect to before.
The e-type and variance maps are based on 100 realizations.
In all panels, the interpretation of the seismic data, and the buffer zone around the Tønder model are explicitly shown in terms of sand and clay (the red homogeneous volumes represent the sand bodies, the blue volumes show the clay lenses). Vertical exaggeration = 20x